ACS Energy Letters

http://pubs.acs.org/journal/aelccp

LETTER

All-Perovskite Tandem Solar Cells Approach 26.5% Efficiency by Employing Wide Bandgap Lead Perovskite Solar Cells with New Monomolecular Hole Transport Layer

Huan Bi,* Jiaqi Liu, Zheng Zhang, Liang Wang, Raminta Beresneviciute, Daiva Tavgeniene, Gaurav Kapil, Chao Ding, Ajay Kumar Baranwal, Shahrir Razey Sahamir, Yoshitaka Sanehira, Hiroshi Segawa,* Saulius Grigalevicius,* Qing Shen,* and Shuzi Hayase*

Cite This: ACS Energy Lett. 2023, 8, 3852−3859

Read Online

ACCESS | Metrics & More | Article Recommendations | Supporting Information

ABSTRACT: **Self-assembled molecules (SAMs) have been widely employed as hole transport layers (HTLs) that can improve the power conversion efficiency (PCE) of perovskite solar cells (PSCs). However, few SAMs are effective for wide band gap (WBG; E_g = 1.77 eV) PSCs. We found that [3-[4-(diphenylamino)phenyl]-9H-carbazol-9-yl]propylphosphonic acid (4dp3PACz) working as a monomolecular HTL is effective for WPG ($FA_{0.8}Cs_{0.2}PbI_{1.8}Br_{1.2}$) PSCs. The 4dp3PACz improved the quality of the perovskite film and reduced the defect density of the film, which reduced the nonradiative recombination and enhanced the carrier transport. 17.17% efficiency is reported. In addition, all-perovskite tandem solar cells consisting of the WBG PSC as the top cell gave 26.47% efficiency.**

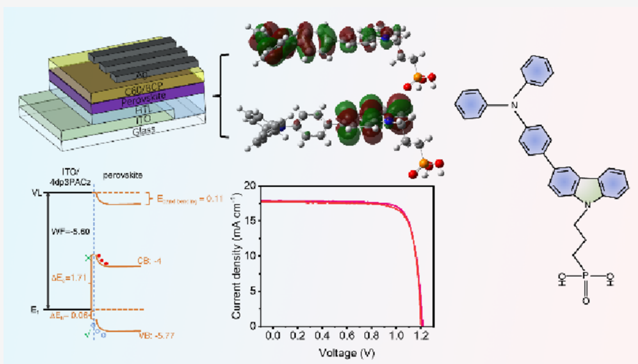

Perovskite solar cells (PSCs) have recently progressed due to their long carrier lifetime, tunable bandgap, and matched optical absorption.[1,2] As reported, the power conversion efficiency (PCE) of the single-junction PSCs has achieved 25.7%, comparable with that of silicon solar cells (Si-PSCs).[3−6] In order to pursue further high efficiency, perovskite tandem solar cells have attracted interest. The all-perovskite tandem solar cell is one type of perovskite tandem solar cells and has the potential to be fabricated on flexible plastic films.[7,8]

All-perovskite tandem solar cells consist of narrow band gap PSCs (NBG PSCs) and wide band gap PSCs (WBG PSCs). Many works have been performed to explore the NBG PSCs consisting of a Sn/Pb alloyed perovskite layer, and an efficiency of 23−24% has been reported.[9] The efficiency enhancement of the WBG PSCs is another important item. Since the band gap of the Sn/Pb perovskite solar cells is about 1.2 eV, the band gap of the top PSC layer must be about 1.7−1.8 eV.[10] We selected $FA_{0.8}Cs_{0.2}PbI_{1.8}Br_{1.2}$ as the top layer.[10−14] It is well-known that poly[bis(4-phenyl)(2,4,6-trimethylphenyl)amine] (PTAA) is a representative hole transport layer (HTL).[15−17] However, the perovskite cannot be well contacted on its surface because of its hydrophobicity. Because of this, a poor perovskite film forms. Tan and co-workers used nickel oxide nanoparticles (NiOx) as the HTL for $FA_{0.8}Cs_{0.2}PbI_{1.8}Br_{1.2}$ (WBG) solar cells, and they achieved a 16.4% efficiency.[18] At the same time, they used cross-linked materials as the HTL and reported a PCE of 16.7% on $FA_{0.8}Cs_{0.2}PbI_{1.8}Br_{1.2}$ solar cells.[10]

Self-assembled monomolecular (SAMs) layers are useful as the HTL for high-efficiency PSCs, such as $CH_3NH_3PbI_3$-, $Cs_{0.05}MA_{0.15}FA_{0.80}PbI_3$-, or $FA_{0.8}Cs_{0.2}PbI_{1.8}Br_{1.2}$-based PSCs, organic solar cells, and so on.[19−22] These molecules have p-type molecular groups, linker groups, and anchor groups. Phosphoryl groups are widely used as anchor groups.[20] For example, Janssen's group utilized (3-(9H-carbazol-9-yl)-

Received: June 27, 2023
Accepted: August 21, 2023

https://doi.org/10.1021/acsenergylett.3c01275
ACS Energy Lett. 2023, 8, 3852−3859

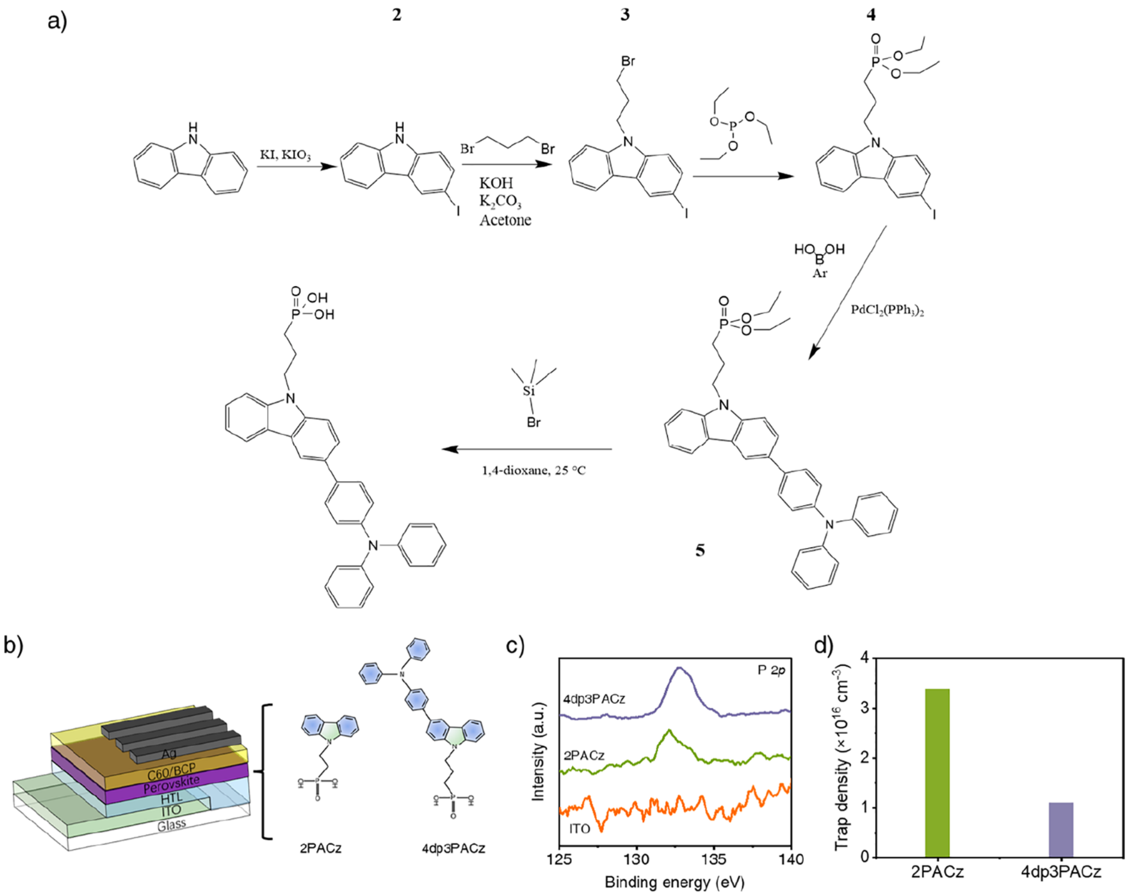

Figure 1. (a) Synthetic route of 4dp3PACz. (b) Structure of the PSCs and the molecular structure used for ITO surface modification. (c) P 2*p* XPS signal of the ITO with or without the monomolecular layer. (d) The defect density of the perovskite film deposited on 2PACz or 4dp3PACz with a hole-only device (ITO/4dp3PACz/perovskite/Spiro-OMeTAD/Ag or ITO/2PACz/perovskite/Spiro-OMeTAD/Ag, calculated from the SCLC result).

propyl)phosphonic acid (3PACz) as the hole transport layer (HTL) for organic solar cells, achieving a reported PCE of 17.4%. This PCE is higher than the 16.2% achieved by solar cells with PEDOT: PSS as the HTL.[23] They argued that all PACz monolayer HTLs demonstrate superior optical transmittance and lower electrical resistance compared to those of PEDOT:PSS. These characteristics are beneficial for improving photovoltaic parameters. Moreover, the 3PACz-based device exhibited a lower film defect density, higher carrier transport efficiency, and lower interfacial recombination, further contributing to its enhanced performance. Our previous work also demonstrated that 3PACz-based molecules can effectively improve the performance of devices.[24] On the other hand, triarylamine-based conjugated polymers have been widely used as HTLs for inverted PSCs, with various molecular designs based on triarylamine being extensively reported.[25−27] Sonar et al. designed and synthesized a series of triphenylamine-functionalized molecules as HTLs, achieving an efficiency of 15.9% and demonstrating excellent stability.[28] In conclusion, 3PACz has been shown to have good application prospects compared to 2PACz or 4PACz, and meanwhile, the triarylamine is also regarded as a functional group that can effectively improve the performance of materials. In this work, the solar cell performance of solar cells with newly developed 3-[3-[4-(diphenylamino)phenyl]-9H-carbazol-9-yl]-propylphosphonic acid (4dp3PACz) as the HTL is discussed. We report 17.17% and 26.47% efficiency for the WBG-PSCs and the all-perovskite tandem solar cells by employing the newly developed HTL.

The synthesis of substituted carbazole-based SAM materials was carried out by a synthetic route, as shown in Figure 1a. A procedure Tucker first obtained was 3-Iodo-9H-carbazole (**2**).[29] Then, the **2** was alkylated under basic conditions using an excess of 1,3-bromopropane to produce 9-(3-bromopropyl)-3-iodo-9H-carbazole (**3**).[30] In the third step, through the Arbuzov reaction, the aliphatic bromide was transformed into key starting material, phosphonic acid ethyl ester (**4**). Intermediate materials (**5**) were then prepared by the Ullmann coupling reaction of the iodo-compound (**4**) with an excess of 4-(diphenylamino)phenylboronic acid. The mentioned reaction was carried out in tetrahydrofuran (THF) using $PdCl_2(PPh_3)_2$ as a catalytic system. The objective compounds as phosphonic acids 4dp3PACz were finally prepared by ester hydrolysis of the phosphonates (**5**) by using bromotrimethylsilane. 1H-NMR and ^{13}C-NMR spectroscopy were used to confirm the structure of the intermediate 4dp3PACz and are shown in Figures S1 and S2. Differential scanning calorimetry (DSC, Figure S3) reveals that the 4dp3PACz has good thermal stability.

The device structure used in this work is ITO/HTL/perovskite/C60/BCP/Ag, as shown in Figure 1b. X-ray photoelectron spectroscopy (XPS) was measured to prove the existence of SAMs on ITO. After the 4dp3PACz was spin-coated, the substrate was washed with DMF solution.

https://doi.org/10.1021/acsenergylett.3c01275
ACS Energy Lett. 2023, 8, 3852−3859

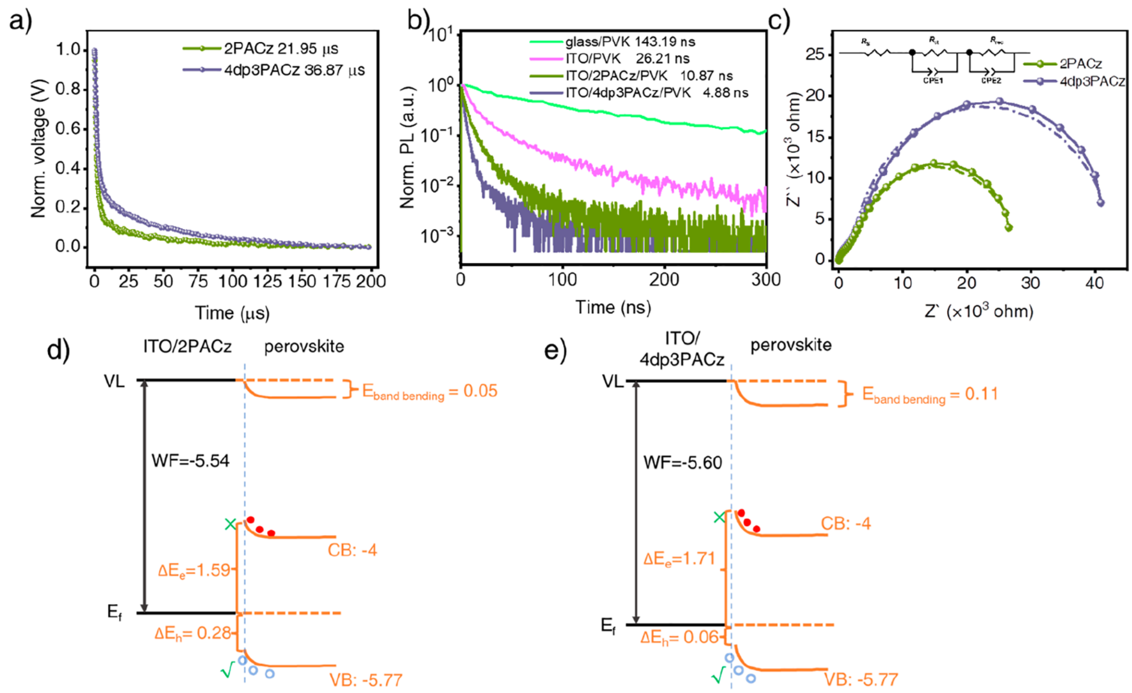

Figure 2. (a) TPV curves for the device with 2PACz or 4dp3PACz as HTL. (b) TRPL curves of the perovskite films deposited on glass, ITO, ITO/2PACz, and ITO/4dp3PACz. (c) Nyquist plots of the control device and target device measured at the frequency ranging from 1 MHz to 10 Hz with a bias V_{OC}. Band bending of (d) ITO/2PACz/PVK and (e) ITO/4dp3PACz/PVK.

Therefore, only the molecules bonded on the ITO should remain on the substrate, and others are removed from the ITO surface.[22] As shown in Figure 1c, a P 2p signal was observed on the ITO treated with 4dp3PACz, while not on the bare ITO. This result shows that the 4dp3PACz is on the ITO. As presented in Figure S4, the XPS peak of In 3d of the ITO shifted after 4dp3PACz and 2PACz were deposited. The shift of the 4dp3PACz treatment was larger than that of the 2PACz treatment. According to previous work, this shift proves the chemical bonding between ITO and the adsorbed molecules.[9,31]

UV−vis absorption was used to determine the perovskite bandgap. As shown in Figure S5, the calculated bandgap using the Tauc plot was 1.77 eV, which was wider than that of the $FASnI_3$ (1.4 eV).[14,18] It has been reported that the perovskite film quality is affected by the hydrophilic properties of the substrate surface. The water contact angle on the substrate was used to study the hydrophilicity.[32−34] Figure S6 shows that ITO/4dp3PACz (55°) shows a smaller contact angle than ITO/2PACz (64°). It is expected that the former gives better perovskite film than the latter. Scanning electron microscopy (SEM) measurement was carried out to study the morphology of perovskite films. As shown in Figure S7, the perovskite thin film deposited on 4dp3PACz has fewer pinholes than the film deposited on 2PACz. The improved film morphology of the former may be due to the better hydrophilicity of the 4dp3PACz film.[2,35] XRD patterns were further employed to study the effect of the perovskite film crystal structure (Figure S8). As shown in Figure S8a, the diffraction peak position of the perovskite film on 4dp3PACz was the same as that on 2PACz. The crystal size of the perovskite film on ITO/4dp3PACz calculated from the fwhm was 47.91 nm, which was larger than that on the ITO/2PACz (41.47 nm).

Space charge limited current (SCLC) measurements were performed to calculate the defect densities of the perovskite films. The hole-only device with the structure of ITO/monomolecular layer/perovskite/Spiro-OMeTAD/Ag was prepared, and the dark current−voltage (I−V) curve is shown in Figure 1d and Figure S9. The defect density was calculated by the equation $n_t = (2\varepsilon\varepsilon_0 V_{TFL})/(eL^2)$,[36] where ε is the dielectric constant of the perovskite, e is the elementary charge, L is the thickness film of the perovskite, and ε_0 is the vacuum dielectric constant. The perovskite film defect density of the ITO/2PACz/perovskite/Spiro-OMeTAD/Ag structure was estimated to be 3.37×10^{16} cm^{-3}, which was higher than the defect density of 1.10×10^{16} cm^{-3} observed in the ITO/4dp3PACz/perovskite/Spiro-OMeTAD/Ag structure. Furthermore, to assess the impact of excess aromatic rings on film defects, we fabricated hole-only devices using 3PACz as the HTL. Figure S10 shows that the 3PACz-based film had a defect density of 1.48×10^{16} cm^{-3}, which is higher than the defect density of the 4dp3PACz-based film (1.10×10^{16} cm^{-3}). Previous reports have indicated that benzene rings can effectively passivate defects in the perovskite film, leading to an improvement in the film's quality.[37−40]

Besides perovskite film quality, efficient charge transfer, and less nonradiative recombination are also beneficial for improving the device's performance. Transient photovoltage (TPV) was performed to study the nonradiative recombination in the device structure of ITO/2PACz or 4dp3PACz/perovskite/C60/BCP/Ag.[41,42] As shown in Figure 2a, the carrier lifetimes of the device increased from 21.95 μs (the solar cell with 2PACz) to 36.87 μs (the solar cell with 4dp3PACz), which proves that the nonradiative recombination of the device with 4dp3PACz was suppressed, compared with the device with 2PACz. The ideality factor (n) is a tool to evaluate the recombination in PSCs.[43] As exhibited in Figure S11, the device with 4dp3PACz exhibited a lower n of 1.43, compared with the device with 2PACz(1.93), which indicates mitigated nonradiative recombination in the device with

https://doi.org/10.1021/acsenergylett.3c01275
ACS Energy Lett. 2023, 8, 3852−3859

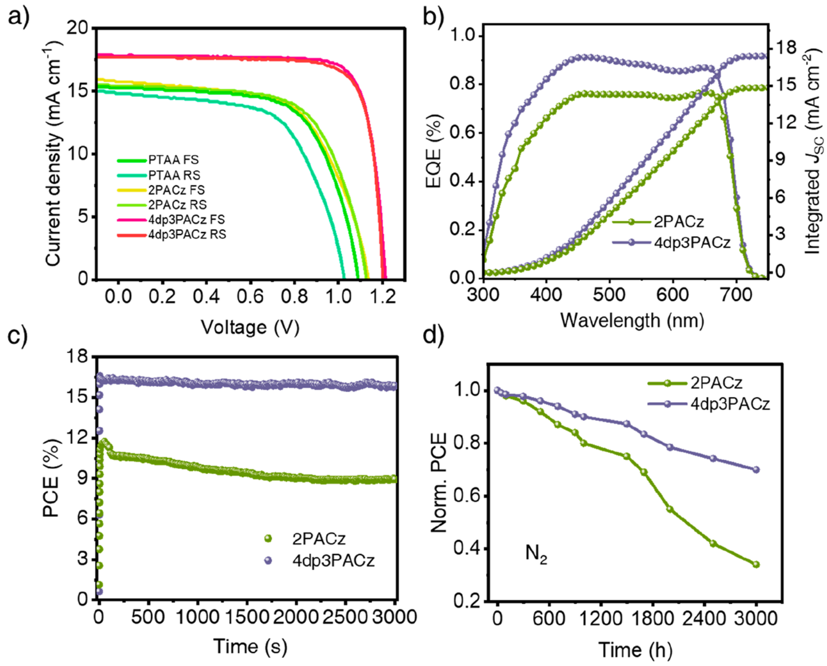

Figure 3. (a) Champion forward- and reverse-scanned *J*−*V* characteristics of the PV with PTAA-, 2PACz-, and 4dp3PACz. (b) Champion IPCE of the device with 2PACz and 4dp3PACz. (c) MPPT test results and (d) long-term stability test of the device with 2APCz and 4dp3PACz as HTL.

4dp3PACz. The device structure's time-resolved photoluminescence (TRPL) with ITO/SAMs/perovskite was measured to uncover carrier transfer from the perovskite layer to HTLs. As shown in Figure 2b, TRPL spectra were fitted by the double-exponential function equation of $I(t) = I_0 + A_1\exp(-t/\tau_1) + A_2\exp(-t/\tau_2)$, where A_1 and A_2 represent the decay amplitude of fast and slow decay process, respectively. τ_1 and τ_2 are the fast and slow decay time constants, respectively.[44] The average carrier lifetime (τ_{ave}) was calculated using the equation $\tau_{ave} = (A_1\tau_1^2 + A_2\tau_2^2)/(A_1\tau_1 + A_2\tau_2)$. The perovskite film deposited on the glass shows a τ_{ave} value of 143.19 ns. The perovskite film deposited on 2PACz gave a τ_{ave} of 10.87 ns, while the one deposited on 4dp3PACz showed a τ_{ave} of 4.88 ns. The results show that the hole collection from the perovskite layer to 4dp3PACz is faster than 2PACz. In order to remove the influence of the substrate, we evaluated the carrier lifetime with the structure of ITO/PVK, and the results showed that the perovskite film deposited on ITO gave a τ_{ave} of 26.21 ns. Figure 2c shows the Nyquist plots of the devices with 2PACz or 4dp3PACz as HTL. ITO/2PACz or 4dp3PACz/perovskite/C60/BCP/Ag impedance was measured at an open-circuit voltage (V_{OC}) in the frequency range of 1 MHz to 10 Hz. The fitting circuit is shown in the inset. As shown in Table S1, the semicircle at the high-frequency region was ascribed to charge transfer resistance (R_{ct}), and the semicircle at the low-frequency region was attributed to recombination resistance (R_{rec}).[45] The R_{ct} decreased when 4dp3PACz was used as HTL, while the R_{rec} increased, concluding that 4dp3PACz is conducive to transporting carriers while inhibiting the recombination of carriers.

The energy level diagrams of the ITO/2PACz or ITO/4dp3PACz and the perovskite are shown in Figure 2d,e. The Fermi level was determined using Kelvin probe measurements (Table S2), while the energy levels were detected through photoelectron yield spectroscopy (PYS) as shown in Figure S12. After the contact, the Fermi level (E_f) of ITO/2PACz/perovskite and ITO/4dp3PACz/perovskite became −5.54 and −5.60 eV, respectively. The band bending of the conduction band (CB) and the balance band (VB) for the latter was bigger than that of the former, suggesting that the charge recombination of the latter is suppressed while the charge transport is facilitated, compared to that of the former.[46]

Figure 3a shows the best *J*−*V* curves of the solar cell with 2PACz and 4dp3PACz, respectively. The corresponding photovoltaic parameters are summarized in Table S3. Figure S13 summarizes the statistics of the photovoltaic performance of the solar cells with 2PACz and 4pd3PACz as the HTL. In Figure 3a and Table S3, the device with PTAA, a widely employed material for the HTL,[47,48] is also added as the reference. Compared with PTAA and 2PACz, 4dp3PACz exhibited higher photovoltaic performance. WBG PSCs with 4dp3PACz have an average PCE of 17.17%, a short-circuit current density (J_{SC}) of 17.8 mA cm^{-2}, a V_{OC} of 1.214 V, and a fill factor (FF) of 79.44%. The PSCs with 2PACz showed a PCE of 11.68% with a J_{SC} of 15.9 mA cm^{-2}, a V_{OC} of 1.132 V, and an FF of 60.89%. Additionally, we investigated the use of 3APCz as the HTL to understand the impact of extra benzene rings on device performance. Figure S14 illustrates that compared to 4dp3PACz, PSCs based on 3PACz exhibit a lower PCE. The improved PCE can be attributed to the enhanced quality of the perovskite film (as shown in Figure S10). To further elucidate the differences between 3PACz and 4dp3PACz, density functional theory (DFT) calculations were conducted. Figure S15 reveals that both the 3PACz/perovskite and 4dp3PACz/perovskite structures exhibit obvious charge transfer. However, 4dp3PACz demonstrates a lower binding energy, indicating a more stable binding between 4dp3PACz and the perovskite. This stability is attributed to the presence of an excess of benzene rings in 4dp3PACz.[37−40]

The improved performance is attributed to improved film quality, reduced nonradiative recombination, and enhanced carrier transfer.[49] Incident photon-to-current conversion

https://doi.org/10.1021/acsenergylett.3c01275
ACS Energy Lett. 2023, 8, 3852−3859

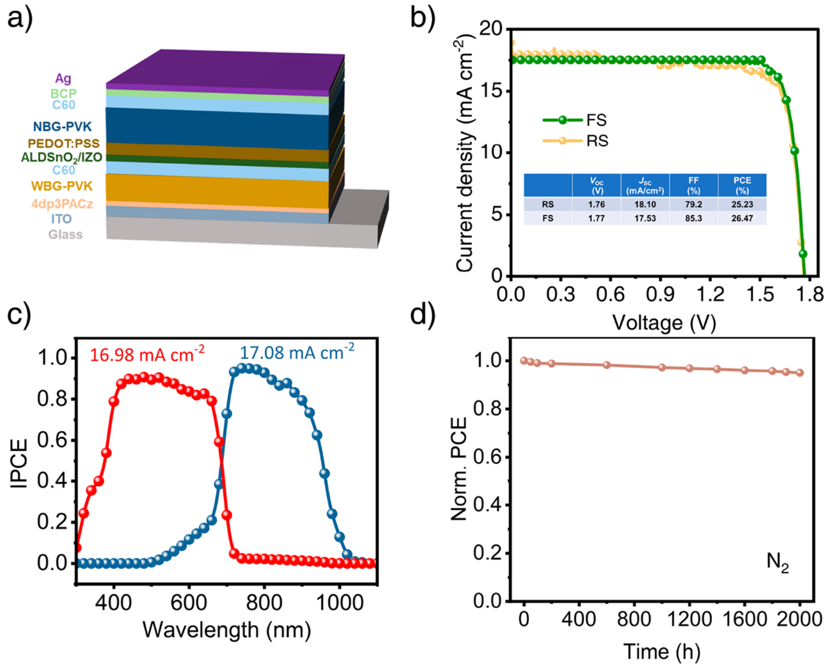

Figure 4. (a) The structure of all-perovskite tandem solar cells used in this work. (b) *J*−*V* curves and (c) IPCE of the device with 4dp3PACz as HTL. (d) Stability of the unencapsulated tandem PSCs aged in the nitrogen-filled glovebox.

efficiency (IPCE) spectra of the device with 2PACz or 4dp3PACz as the HTL are shown in Figure 3b. The integrated current agrees well with J_{SC}. Another reason is the high hole mobility of the 4dp3PACz (Figure S16).[45,50,51] By using maximum power point tracking (MPPT) under one sun illumination, we recorded the efficiency, as shown in Figure 3c. The stability of the device with 4dp3PACz was better than that with 2PACz. As shown in Figure 3d, the efficiency of the encapsulated device with 2PACz decreased to 30% of its initial PCE after 3000 h. In contrast, the device with 4dp3PACz as the HTL retained 70% of its original PCE after the same aging period.

The perovskite/perovskite tandem solar cell was fabricated to show the potential of the 4dp3PACz. Figure 4a shows the structure ITO/SAMs/WBG perovskite($FA_{0.8}Cs_{0.2}PbI_{1.8}Br_{1.2}$)/C60/ALD SnO_2/IZO/PEDOT:PSS/NBG perovskite-($Cs_{0.025}FA_{0.475}MA_{0.5}Sn_{0.5}Pb_{0.5}I_{2.925}Br_{0.075}$)/C60/BCP/Ag. The typical *J*−*V* curves of the best-performing tandem solar cells with 4dp3PACz are shown in Figure 4b. After using 4dp3PACz, we observed a PCE of 26.47% with a J_{SC} of 17.53 mA cm^{-2}, a V_{OC} of 1.77 V, and an FF of 85.3%. Figure 4c shows the IPCE curves of the tandem solar cell. The integrated current corresponded to the *J*−*V* curves. Figure S17 presents the *J*−*V* curves and IPCE test results for the narrow-band gap perovskite used in this study. Additionally, the stability of the unpackaged device was assessed. Figure S18 displays the MPPT results of the tandem solar cells with 4dp3PACz as the HTL. Even after 7000 s, the device maintains a stable output efficiency. Furthermore, Figure 4d demonstrates that after 2000 h of aging, the device still retains 95% of its initial efficiency, indicating the excellent potential of 4dp3PACz as a commercially viable HTL.

We have proved that the monomolecular layer of 4dp3PACz works as the hole transport layer better than the previously reported 2PACz and PTAA. The perovskite layer fabricated on 4dp3PACz had better quality, such as less carrier trap density, longer carrier lifetime, and large charge recombination resistance, probably because of the hydrophilic properties of the 4dp3PACz. Meanwhile, −4dp also can effectively passivate defects in thin films. The WBG PSCs (1.77 eV bandgap) with 17.17% yield were prepared. In addition, all-perovskite/perovskite tandem solar cells with 26.47% were reported by coupling the WBG device with 1.77 eV bandgap and 1.25 eV NBG device.

■ ASSOCIATED CONTENT

Supporting Information

The Supporting Information is available free of charge at https://pubs.acs.org/doi/10.1021/acsenergylett.3c01275.

Experimental Section (including materials, device fabrication, and characterization); NMR spectrum and DCS curves of 4dp3PACz; XPS patterns, Tauc plot, water contact angle, SEM images, SCLC curves, PYS spectra, Mott−Schottky plot, statistical diagrams of photovoltaic parameters, DFT result, and hole mobility of the different HTLs (PDF)

■ AUTHOR INFORMATION

Corresponding Authors

Huan Bi − *i-Powered Energy System Research Center (i-PERC) and Graduate School of Informatics and Engineering, The University of Electro-Communications, Chofu, Tokyo 182-8585, Japan*; orcid.org/0000-0001-7680-9816; Email: hbi.trans.sci@gmail.com

Hiroshi Segawa − *Research Center for Advanced Science and Technology, The University of Tokyo, Meguro-ku, Tokyo 153-8904, Japan*; orcid.org/0000-0001-8076-9722; Email: csegawa@mail.ecc.u-tokyo.ac.jp

Saulius Grigalevicius − *Department of Polymer Chemistry and Technology, Kaunas University of Technology, LT50254 Kaunas, Lithuania*; Email: saulius.grigalevicius@ktu.lt

Qing Shen − *i-Powered Energy System Research Center (i-PERC) and Graduate School of Informatics and Engineering,* *The University of Electro-Communications, Chofu, Tokyo 182-8585, Japan;* orcid.org/0000-0001-8359-3275; Email: shen@pc.uec.ac.jp

Shuzi Hayase − *i-Powered Energy System Research Center (i-PERC) and Graduate School of Informatics and Engineering, The University of Electro-Communications, Chofu, Tokyo 182-8585, Japan;* orcid.org/0000-0001-8192-5336; Email: hayase@uec.ac.jp

Authors

Jiaqi Liu − *i-Powered Energy System Research Center (i-PERC), The University of Electro-Communications, Chofu, Tokyo 182-8585, Japan*

Zheng Zhang − *i-Powered Energy System Research Center (i-PERC), The University of Electro-Communications, Chofu, Tokyo 182-8585, Japan*

Liang Wang − *i-Powered Energy System Research Center (i-PERC), The University of Electro-Communications, Chofu, Tokyo 182-8585, Japan*

Raminta Beresneviciute − *Department of Polymer Chemistry and Technology, Kaunas University of Technology, LT50254 Kaunas, Lithuania*

Daiva Tavgeniene − *Department of Polymer Chemistry and Technology, Kaunas University of Technology, LT50254 Kaunas, Lithuania*

Gaurav Kapil − *i-Powered Energy System Research Center (i-PERC), The University of Electro-Communications, Chofu, Tokyo 182-8585, Japan*

Chao Ding − *Graduate School of Informatics and Engineering, The University of Electro-Communications, Chofu, Tokyo 182-8585, Japan; Institute of New Energy and Low-Carbon Technology, Sichuan University, Chengdu 610065, China*

Ajay Kumar Baranwal − *i-Powered Energy System Research Center (i-PERC), The University of Electro-Communications, Chofu, Tokyo 182-8585, Japan;* orcid.org/0000-0003-4582-4532

Shahrir Razey Sahamir − *i-Powered Energy System Research Center (i-PERC), The University of Electro-Communications, Chofu, Tokyo 182-8585, Japan;* orcid.org/0000-0002-9167-5980

Yoshitaka Sanehira − *i-Powered Energy System Research Center (i-PERC), The University of Electro-Communications, Chofu, Tokyo 182-8585, Japan;* orcid.org/0000-0003-2030-2690

Complete contact information is available at: https://pubs.acs.org/10.1021/acsenergylett.3c01275

Notes

The authors declare no competing financial interest.

■ ACKNOWLEDGMENTS

This work was financially supported by the NEDO project. This work was also supported by project S-LJB-22-2 from the Research Council of Lithuania.

■ REFERENCES

(1) Bi, H.; Han, G.; Guo, M.; Ding, C.; Zou, H.; Shen, Q.; Hayase, S.; Hou, W. Multistrategy Preparation of Efficient and Stable Environment-Friendly Lead-Based Perovskite Solar Cells. *ACS Appl. Mater. Interfaces* **2022**, *14*, 35513.

(2) Bi, H.; Guo, Y.; Guo, M.; Ding, C.; Hayase, S.; Mou, T.; Shen, Q.; Han, G.; Hou, W. Highly Efficient and Low Hysteresis Methylammonium-Free Perovskite Solar Cells Based on Multifunctional Oteracil Potassium Interface Modification. *Chem. Eng. J.* **2022**, *439*, No. 135671.

(3) Park, J.; Kim, J.; Yun, H.-S.; Paik, M. J.; Noh, E.; Mun, H. J.; Kim, M. G.; Shin, T. J.; Seok, S. I. Controlled Growth of Perovskite Layers with Volatile Alkylammonium Chlorides. *Nature* **2023**, *616*, 724.

(4) Zhou, Y.; Herz, L. M.; Jen, A. K. Y.; Saliba, M. Advances and Challenges in Understanding the Microscopic Structure−Property−Performance Relationship in Perovskite Solar Cells. *Nat. Energy* **2022**, *7*, 794.

(5) Sharma, R.; Sharma, A.; Agarwal, S.; Dhaka, M. S. Stability and Efficiency Issues, Solutions and Advancements in Perovskite Solar Cells: A Review. *Sol. Energy* **2022**, *244*, 516.

(6) Zhang, D.; Li, D.; Hu, Y.; Mei, A.; Han, H. Degradation Pathways in Perovskite Solar Cells and How to Meet International Standards. *Commun. Mater.* **2022**, *3*, 58.

(7) Zhao, D.; Chen, C.; Wang, C.; Junda, M. M.; Song, Z.; Grice, C. R.; Yu, Y.; Li, C.; Subedi, B.; Podraza, N. J.; Zhao, X.; Fang, G.; Xiong, R.-G.; Zhu, K.; Yan, Y. Efficient Two-Terminal All-Perovskite Tandem Solar Cells Enabled by High-Quality Low-Bandgap Absorber Layers. *Nat. Energy* **2018**, *3*, 1093.

(8) Palmstrom, A. F.; Eperon, G. E.; Leijtens, T.; Prasanna, R.; Habisreutinger, S. N.; Nemeth, W.; Gaulding, E. A.; Dunfield, S. P.; Reese, M.; Nanayakkara, S.; Moot, T.; Werner, J.; Liu, J.; To, B.; Christensen, S. T.; McGehee, M. D.; van Hest, M. F. A. M.; Luther, J. M.; Berry, J. J.; Moore, D. T. Enabling Flexible All-Perovskite Tandem Solar Cells. *Joule* **2019**, *3*, 2193.

(9) Kapil, G.; Bessho, T.; Sanehira, Y.; Sahamir, S. R.; Chen, M.; Baranwal, A. K.; Liu, D.; Sono, Y.; Hirotani, D.; Nomura, D.; Nishimura, K.; Kamarudin, M. A.; Shen, Q.; Segawa, H.; Hayase, S. Tin−Lead Perovskite Solar Cells Fabricated on Hole Selective Monolayers. *ACS Energy Lett.* **2022**, *7*, 966.

(10) Wang, Y.; Gu, S.; Liu, G.; Zhang, L.; Liu, Z.; Lin, R.; Xiao, K.; Luo, X.; Shi, J.; Du, J.; Meng, F.; Li, L.; Liu, Z.; Tan, H. Cross-Linked Hole Transport Layers for High-Efficiency Perovskite Tandem Solar Cells. *Sci. China Chem.* **2021**, *64*, 2025.

(11) Jiang, Q.; Tong, J.; Scheidt, R. A.; Wang, X.; Louks, A. E.; Xian, Y.; Tirawat, R.; Palmstrom, A. F.; Hautzinger, M. P.; Harvey, S. P.; Johnston, S.; Schelhas, L. T.; Larson, B. W.; Warren, E. L.; Beard, M. C.; Berry, J. J.; Yan, Y.; Zhu, K. Compositional Texture Engineering for Highly Stable Wide-bandgap Perovskite Solar Cells. *Science* **2022**, *378*, 1295.

(12) Yu, Z.; Chen, X.; Harvey, S. P.; Ni, Z.; Chen, B.; Chen, S.; Yao, C.; Xiao, X.; Xu, S.; Yang, G.; Yan, Y.; Berry, J. J.; Beard, M. C.; Huang, J. Gradient Doping in Sn-Pb Perovskites by Barium Ions for Efficient Single-Junction and Tandem Solar Cells. *Adv. Mater.* **2022**, *34*, No. 2110351.

(13) Wen, J.; Zhao, Y.; Liu, Z.; Gao, H.; Lin, R.; Wan, S.; Ji, C.; Xiao, K.; Gao, Y.; Tian, Y.; Xie, J.; Brabec, C. J.; Tan, H. Steric Engineering Enables Efficient and Photostable Wide-Bandgap Perovskites for All-perovskite Tandem Solar Cells. *Adv. Mater.* **2022**, *34*, No. 2110356.

(14) Brinkmann, K. O.; Becker, T.; Zimmermann, F.; Kreusel, C.; Gahlmann, T.; Theisen, M.; Haeger, T.; Olthof, S.; Tuckmantel, C.; Gunster, M.; Maschwitz, T.; Gobelsmann, F.; Koch, C.; Hertel, D.; Caprioglio, P.; Pena-Camargo, F.; Perdigon-Toro, L.; Al-Ashouri, A.; Merten, L.; Hinderhofer, A.; Gomell, L.; Zhang, S.; Schreiber, F.; Albrecht, S.; Meerholz, K.; Neher, D.; Stolterfoht, M.; Riedl, T. Perovskite-organic Tandem Solar Cells with Indium Oxide Interconnect. *Nature* **2022**, *604*, 280.

(15) Farokhi, A.; Shahroosvand, H.; Monache, G. D.; Pilkington, M.; Nazeeruddin, M. K. The Evolution of Triphenylamine Hole Transport Materials for Efficient Perovskite Solar Cells. *Chem. Soc. Rev.* **2022**, *51*, 5974.

(16) Wang, Y.; Duan, L.; Zhang, M.; Hameiri, Z.; Liu, X.; Bai, Y.; Hao, X. Ptaa as Efficient Hole Transport Materials in Perovskite Solar Cells: A Review. *Sol. RRL* **2022**, *6*, No. 2200234.

(17) Li, Y.; Liao, J.-F.; Pan, H.; Xing, G. Interfacial Engineering for High-Performance PTAA-based Inverted 3D Perovskite Solar Cells. *Sol. RRL* **2022**, *6*, No. 2200647.
(18) Xiao, K.; Lin, R.; Han, Q.; Hou, Y.; Qin, Z.; Nguyen, H. T.; Wen, J.; Wei, M.; Yeddu, V.; Saidaminov, M. I.; Gao, Y.; Luo, X.; Wang, Y.; Gao, H.; Zhang, C.; Xu, J.; Zhu, J.; Sargent, E. H.; Tan, H. All-perovskite Tandem Solar Cells with 24.2% Certified Efficiency and Area over 1 Cm^2 Using Surface-Anchoring Zwitterionic Antioxidant. *Nat. Energy* **2020**, *5*, 870.
(19) Guan, L.; Yu, L.; Wu, L.; Zhang, S.; Lin, Y.; Jiao, Y.; Zhang, S.; Zhao, F.; Ren, Y.; Zhou, X.; Liu, Z. Grain Size Control of Perovskite Films Based on *B*-Alanine Self-Assembled Monolayers Surface Treatment. *Thin Solid Films* **2021**, *732*, No. 138770.
(20) Ali, F.; Roldán-Carmona, C.; Sohail, M.; Nazeeruddin, M. K. Applications of Self-Assembled Monolayers for Perovskite Solar Cells Interface Engineering to Address Efficiency and Stability. *Adv. Energy Mater.* **2020**, *10*, No. 2002989.
(21) Lin, Y.; Zhang, Y.; Zhang, J.; Marcinskas, M.; Malinauskas, T.; Magomedov, A.; Nugraha, M. I.; Kaltsas, D.; Naphade, D. R.; Harrison, G. T.; El-Labban, A.; Barlow, S.; De Wolf, S.; Wang, E.; McCulloch, I.; Tsetseris, L.; Getautis, V.; Marder, S. R.; Anthopoulos, T. D. 18.9% Efficient Organic Solar Cells Based on N-Doped Bulk-Heterojunction and Halogen-Substituted Self-assembled Monolayers as Hole Extracting Interlayers. *Adv. Energy Mater.* **2022**, *12*, No. 2202503.
(22) Deng, X.; Qi, F.; Li, F.; Wu, S.; Lin, F. R.; Zhang, Z.; Guan, Z.; Yang, Z.; Lee, C. S.; Jen, A. K. Co-Assembled Monolayers as Hole-Selective Contact for High-performance Inverted Perovskite Solar Cells with Optimized Recombination Loss and Long-Term Stability. *Angew. Chem.* **2022**, *61*, No. 202203088.
(23) Bin, H.; Datta, K.; Wang, J.; van der Pol, T. P. A.; Li, J.; Wienk, M. M.; Janssen, R. A. J. Finetuning Hole-extracting Monolayers for Efficient Organic Solar Cells. *ACS Appl. Mater. Interfaces* **2022**, *14*, 16497.
(24) Beresneviciute, R.; Bi, H.; Liu, J.; Kapil, G.; Tavgeniene, D.; Zhang, Z.; Wang, L.; Ding, C.; Sahamir, S. R.; Sanehira, Y.; Baranwal, A. K.; Takeshi, K.; Wang, D.; Wei, Y.; Yang, Y.; Kang, D. W.; Grigalevicius, S.; Shen, Q.; Hayase, S. Wide Bandgap Lead Perovskite Solar Cells with Monomolecular Layer from Viewpoint of PTAA Band Bending. *Chemistry and chemical technology: international conference CCT-2023*; Vilnius University Press: Vilnius, 2023; 46. DOI: 10.15388/CCT.2023.
(25) Park, S.; Heo, J. H.; Cheon, C. H.; Kim, H.; Im, S. H.; Son, H. J. A [2,2]paracyclophane Triarylamine-based Hole-transporting Material for High Performance Perovskite Solar Cells. *J. Mater. Chem. A* **2015**, *3*, 24215.
(26) Kim, Y.; Kim, G.; Jeon, N. J.; Lim, C.; Seo, J.; Kim, B. J. Methoxy-functionalized Triarylamine-based Hole-transporting Polymers for Highly Efficient and Stable Perovskite Solar Cells. *ACS Energy Lett.* **2020**, *5*, 3304.
(27) Matsui, T.; Petrikyte, I.; Malinauskas, T.; Domanski, K.; Daskeviciene, M.; Steponaitis, M.; Gratia, P.; Tress, W.; Correa-Baena, J. P.; Abate, A.; Hagfeldt, A.; Gratzel, M.; Nazeeruddin, M. K.; Getautis, V.; Saliba, M. Additive-Free Transparent Triarylamine-based Polymeric Hole-transport Materials for Stable Perovskite Solar Cells. *ChemSusChem* **2016**, *9*, 2567.
(28) Pham, H. D.; Gil-Escrig, L.; Feron, K.; Manzhos, S.; Albrecht, S.; Bolink, H. J.; Sonar, P. Boosting Inverted Perovskite Solar Cell Performance by Using 9,9-Bis(4-Diphenylaminophenyl)Fluorene Functionalized with Triphenylamine as a Dopant-Free Hole Transporting Material. *J. Mater. Chem. A* **2019**, *7*, 12507.
(29) Tucker, S. H. Lxxiv.—Iodination in the Carbazole Series. *J. Chem. Soc.* **1926**, *129*, 546.
(30) Heller, J.; Lyman, D. J.; Hewett, W. A. The Synthesis and Polymerization Studies of Some Higher Homologues of 9-Vinylcarbazole. *Makromo. Chem.* **1964**, 73, 48.
(31) Al-Ashouri, A.; Magomedov, A.; Roß, M.; Jošt, M.; Talaikis, M.; Chistiakova, G.; Bertram, T.; Márquez, J. A.; Köhnen, E.; Kasparavičius, E.; Levcenco, S.; Gil-Escrig, L.; Hages, C. J.; Schlatmann, R.; Rech, B.; Malinauskas, T.; Unold, T.; Kaufmann, C. A.; Korte, L.; Niaura, G.; Getautis, V.; Albrecht, S. Conformal Monolayer Contacts with Lossless Interfaces for Perovskite Single Junction and Monolithic Tandem Solar Cells. *Energy Environ. Sci.* **2019**, *12*, 3356.
(32) Wang, S.; Li, Z.; Zhang, Y.; Liu, X.; Han, J.; Li, X.; Liu, Z.; Liu, S.; Choy, W. C. H. Water-soluble Triazolium Ionic-liquid-induced Surface Self-assembly to Enhance the Stability and Efficiency of Perovskite Solar Cells. *Adv. Funct. Mater.* **2019**, *29*, No. 1900417.
(33) You, J.; Guo, F.; Qiu, S.; He, W.; Wang, C.; Liu, X.; Xu, W.; Mai, Y. The Fabrication of Homogeneous Perovskite Films on Non-wetting Interfaces Enabled by Physical Modification. *J. Energy Chem.* **2019**, *38*, 192.
(34) Xu, C.; Liu, Z.; Lee, E.-C. Stability and Efficiency Improved Perovskite Solar Cells through Tuning the Hydrophobicity of the Hole Transport Layer with an Organic Semiconductor. *J. Mater. Chem. C* **2021**, *9*, 679.
(35) Bi, H.; Zuo, X.; Liu, B.; He, D.; Bai, L.; Wang, W.; Li, X.; Xiao, Z.; Sun, K.; Song, Q.; Zang, Z.; Chen, J. Multifunctional Organic Ammonium Salt-Modified SnO_2 Nanoparticles toward Efficient and Stable Planar Perovskite Solar Cells. *J. Mater. Chem. A* **2021**, *9*, 3940.
(36) Bi, H.; Zuo, X.; Liu, B.; He, D.; Bai, L.; Wang, W.; Li, X.; Xiao, Z.; Sun, K.; Song, Q.; Zang, Z.; Chen, J. Multifunctional Organic Ammonium Salt-Modified Sno2nanoparticles toward Efficient and Stable Planar Perovskite Solar Cells. *J. Mater. Chem. A* **2021**, *9*, 3940.
(37) Bi, H.; Guo, M.; Ding, C.; Hayase, S.; Shen, Q.; Han, G.; Hou, W. A Multifunctional Additive Strategy to Stabilize the Precursor Solution and Passivate Film Defects for Ma-free Perovskite Solar Cells with an Efficiency of 22.75%. *Materials Today Energy* **2023**, *33*, No. 101269.
(38) Xu, Z.; Lu, D.; Liu, F.; Lai, H.; Wan, X.; Zhang, X.; Liu, Y.; Chen, Y. Phase Distribution and Carrier Dynamics in Multiple-Ring Aromatic Spacer-based Two-dimensional Ruddlesden-popper Perovskite Solar Cells. *ACS Nano* **2020**, *14*, 4871.
(39) Zhuang, J.; Mao, P.; Luan, Y.; Yi, X.; Tu, Z.; Zhang, Y.; Yi, Y.; Wei, Y.; Chen, N.; Lin, T.; Wang, F.; Li, C.; Wang, J. Interfacial Passivation for Perovskite Solar Cells: The Effects of the Functional Group in Phenethylammonium Iodide. *ACS Energy Lett.* **2019**, *4*, 2913.
(40) Yang, S.; Dai, J.; Yu, Z.; Shao, Y.; Zhou, Y.; Xiao, X.; Zeng, X. C.; Huang, J. Tailoring Passivation Molecular Structures for Extremely Small Open-circuit Voltage Loss in Perovskite Solar Cells. *J. Am. Chem. Soc.* **2019**, *141*, 5781.
(41) Wolff, C. M.; Caprioglio, P.; Stolterfoht, M.; Neher, D. Nonradiative Recombination in Perovskite Solar Cells: The Role of Interfaces. *Adv. Mater.* **2019**, *31*, No. 1902762.
(42) Ding, C.; Wang, D.; Liu, D.; Li, H.; Li, Y.; Hayase, S.; Sogabe, T.; Masuda, T.; Zhou, Y.; Yao, Y.; Zou, Z.; Wang, R.; Shen, Q. Over 15% Efficiency Pbs Quantum-Dot Solar Cells by Synergistic Effects of Three Interface Engineering: Reducing Nonradiative Recombination and Balancing Charge Carrier Extraction. *Adv. Energy Mater.* **2022**, *12*, No. 2201676.
(43) Bi, H.; Liu, B.; He, D.; Bai, L.; Wang, W.; Zang, Z.; Chen, J. Interfacial Defect Passivation and Stress Release by Multifunctional KPF_6 Modification for Planar Perovskite Solar Cells with Enhanced Efficiency and Stability. *Chem. Eng. J.* **2021**, *418*, No. 129375.
(44) Zhuang, Q.; Wang, H.; Zhang, C.; Gong, C.; Li, H.; Chen, J.; Zang, Z. Ion Diffusion-Induced Double Layer Doping toward Stable and Efficient Perovskite Solar Cells. *Nano Res.* **2022**, *15*, 5114.
(45) Liu, B.; Bi, H.; He, D.; Bai, L.; Wang, W.; Yuan, H.; Song, Q.; Su, P.; Zang, Z.; Zhou, T.; Chen, J. Interfacial Defect Passivation and Stress Release Via Multi-Active-Site Ligand Anchoring Enables Efficient and Stable Methylammonium-Free Perovskite Solar Cells. *ACS Energy Lett.* **2021**, *6*, 2526.
(46) Ullah, A.; Park, K. H.; Lee, Y.; Park, S.; Faheem, A. B.; Nguyen, H. D.; Siddique, Y.; Lee, K. K.; Jo, Y.; Han, C. H.; Ahn, S.; Jeong, I.; Cho, S.; Kim, B.; Park, Y. S.; Hong, S. Versatile Hole Selective Molecules Containing a Series of Heteroatoms as Self-Assembled

Monolayers for Efficient P-I-N Perovskite and Organic Solar Cells. *Adv. Funct. Mater.* **2022**, *32*, No. 2208793.

(47) Huo, X.; Li, Y.; Lu, Y.; Dong, J.; Zhang, Y.; Zhao, S.; Qiao, B.; Wei, D.; Song, D.; Xu, Z. Suppressed Halide Segregation and Defects in Wide Bandgap Perovskite Solar Cells Enabled by Doping Organic Bromide Salt with Moderate Chain Length. *J. Phys. Chem. C* **2022**, *126*, 1711.

(48) Lin, Y.; Chen, B.; Zhao, F.; Zheng, X.; Deng, Y.; Shao, Y.; Fang, Y.; Bai, Y.; Wang, C.; Huang, J. Matching Charge Extraction Contact for Wide-Bandgap Perovskite Solar Cells. *Adv. Mater.* **2017**, *29*, No. 1700607.

(49) Chen, J.; Park, N. G. Causes and Solutions of Recombination in Perovskite Solar Cells. *Adv. Mater.* **2019**, *31*, No. 1803019.

(50) Tavakoli, M. M.; Bi, D.; Pan, L.; Hagfeldt, A.; Zakeeruddin, S. M.; Grätzel, M. Adamantanes Enhance the Photovoltaic Performance and Operational Stability of Perovskite Solar Cells by Effective Mitigation of Interfacial Defect States. *Adv. Energy Mater.* **2018**, *8*, No. 1800275.

(51) Lin, Y.; Shen, L.; Dai, J.; Deng, Y.; Wu, Y.; Bai, Y.; Zheng, X.; Wang, J.; Fang, Y.; Wei, H.; Ma, W.; Zeng, X. C.; Zhan, X.; Huang, J. Π-conjugated Lewis Base: Efficient Trap-passivation and Charge-extraction for Hybrid Perovskite Solar Cells. *Adv. Mater.* **2017**, *29*, No. 1604545.

https://doi.org/10.1021/acsenergylett.3c01275
ACS Energy Lett. 2023, 8, 3852−3859